REPRESENTATIVENESS ERRORS FOR RADIOSONDE OBSERVATIONS

M. Kitchen
Meteorological Office, Bracknell, UK

Summary: Radiosonde observations from the United Kingdom (UK) operational upper air network, as well as from special radiosonde trials, have been analysed to provide statistics of spatial and temporal atmospheric variations. These statistics are applied to a study of the representativeness errors associated with the use of the data in synoptic analysis.

1. INTRODUCTION

Radiosonde measurements are essentially point or line samples along a slant path through the atmosphere. The samples have two undesirable characteristics, namely

a) due to the limited sample volume the data contain information concerning atmospheric variations on time or space scales which are inappropriate to the usage of the data in synoptic meteorology.

b) radiosonde observations are usually ascribed to the launch site location, whereas horizontal displacements for measurements in the upper troposphere and stratosphere are typically several tens of kilometres.

A primary aim of the work ascribed here is to quantify the impact of the sampling characteristics upon the representativeness of the observations and upon the ability of the UK radiosonde network to extract information on the spatial and temporal gradients in the atmospheric fields. In order to meet these aims, statistics of atmospheric variations on scales from a few tens to several hundred kilometres and from a few hours to a few tens of hours were generated. This was accomplished by the analysis of routinely available radiosonde data from stations in the UK. In addition, data have been analysed from a number of special radiosonde trials which were performed in the UK in 1984/5; these trials have provided radiosonde ascent series with smaller time and space separations than is routinely available from the UK operational network.

2. ATMOSPHERIC VARIABILITY STATISTICS

2.1 The Radiosonde Observations

The UK synoptic upper air network consists of 8 radiosonde stations which routinely make full temperature (TEMP) observations at the nominal hours 0000 and 1200 GMT. Additional wind only (PILOT) ascents are performed at 0600 and 1800 GMT. Separation distances between stations in this network are in the range 220-370 km. Another 4 radiosonde stations make observations in support of military test range operations, principally on a demand basis.

The RS3 radiosonde systems at all the UK stations are identical. The radiosonde reports values of temperature every 2 seconds and pressure every 8 seconds. The time constant of the RS3 temperature sensor is extremely short, $<<1$ second in the troposphere and ≤ 1 second at altitudes up to 30 km (see Nash et al, 1985). Temperature measurements at the standard pressure levels are essentially point samples. All stations use a Cossor type 353D radar for windfinding. Horizontal wind measurements attributed to the standard levels represent averages over a period of about 64 seconds, equivalent to a line average over a vertical depth of about 300 m.

Two datasets were assembled which consist of observations at standard pressure levels; one set covers the winter half-year from October 1983 to March 1984 inclusive and the other covers the summer half-year from April to September 1984 inclusive. The 6 month periods were chosen to sustain a compromise between a large data sample in order to achieve statistical reliability, whilst retaining some information upon seasonal differences. The availability of data from the synoptic network is extremely high with only a few ascents missing from each dataset and more than 90% of ascents reach the 50 hPa level.

Spatial variations on the synoptic scale are analysed by comparison of the observations from Crawley with those from the other stations in the synoptic network and temporal variations from consideration of the time series observations from Crawley. Differences between Crawley and Beaufort Park and Crawley and Larkhill are used to extend the analysis to

smaller space scales. The availability of these data is more limited than that for data from the synoptic network. Variability on short time-scales is examined using data from Larkhill and the special trials at Beaufort Park.

2.2 The Analysis Method

Consider two radiosonde observations of a given parameter at the same pressure level. Then the difference between the measurements (Δx) can be written as (see e.g. Morgan, 1984):-

$$\Delta x = x_t + x_s + x_e \qquad 1$$

where x_t is the difference associated with the separation in time of the observations, t, (a function of t only); x_s is the difference associated with the horizontal separation between the observations, s, (a function of s only); and x_e is that part of the difference due to the measurement errors. Squaring and taking the mean over a large set of differences:-

$$\langle \Delta x^2 \rangle = \langle x_t^2 \rangle + \langle x_s^2 \rangle + \langle x_e^2 \rangle + 2(\langle x_t x_s \rangle + \langle x_t x_e \rangle + \langle x_s x_e \rangle) \qquad 2$$

The use of equation 2 was confined to situations where the cross terms could be neglected as being small compared to the other terms. Simplifying the notation, for a given parameter x,

$$\Delta X^2 = \tau_x^2(t) + S_x^2(s) + 2E_x^2 \qquad 3$$

where τ_x is the RMS difference associated with the time separation, S_x is the RMS difference associated with the space separation and $2E_x^2$ is the mean square difference associated with the random components of the radiosonde errors. E_x is therefore the uncertainty associated with each of the radiosonde measurements.

S_x will be derived from the RMS difference between nominally simultaneous radiosonde observations at the same pressure level by radiosondes launched from two stations separated by distance s. The RMS difference can be expressed as:-

$$\Delta X^2 = \tau_x^2(\delta t) + S_x^2(s) + S_x^2(\delta_s) + 2E_x^2 \qquad 4$$

where δt is the small time difference between the nominally simultaneous data due to variations in the launch time and ascent rate of the balloons. δs is the difference between the actual horizontal separation of the observations and the station separation. For the range of s considered here $\delta s \ll s$ and $S_x(\delta s)$ can be neglected as being small

compared to $S_s(s)$ in equation 4. For normal operational practice in the United Kingdom $\delta t < 0.25$ hours and it can be shown that for the range of s considered here. $S_x^2(\delta t)$ is small compared to $S_x^2(s)$.

$\tau_x(t)$ will be derived from a time series of radiosonde observations from a single station. In this case, equation 3 becomes:-

$$\Delta X^2 = \tau_x^2(t) + S_x^2(\delta s(t)) + \tau_x^2(\delta t) + 2E_x^2 \qquad 5$$

δt is here the difference in the actual time separation from the nominal launch time separation, again caused by minor variations in launch time and balloon ascent rates. Changes in the windfield occurring during the time period t between ascents will introduce a horizontal displacement $\delta s(t)$ between the observations. For the range of t considered here $t \gg \delta t$ and $\tau_x(\delta t)$ was neglected. It can also be shown that $S_x^2(\delta s(t)) \ll \tau_x(\delta t)$.

Equations 4 and 5 therefore reduce to:-

for nominally simultaneous ascents, $\Delta X^2 = S_x^2(s) + 2E_x^2$ 6

for time series of ascents, $\Delta X^2 = \tau_x^2(t) + 2E_x^2$ 7

and $S_x(s)$ and $\tau_x(t)$ can thus be obtained from measurements of ΔX and E_x.

For differences between observations separated by up to 1000 km, significant contributions to $S_x(s)$ will arise from climatological mean gradients which are particularly evident in temperature and geopotential. Thus

$$S_x^2 = M_x^2 + F_x^2 \qquad 8$$

where M_x is the mean difference between parameter x at the two locations and F_x is the fluctuating component due to disturbances in the mean gradient. M_x will typically be specific to the two locations and will vary seasonally.

The standard deviations of the standard pressure level observations from Crawley within the summer and winter half year datasets (σ_x) were computed. Values of $\sqrt{2}\sigma_x$ are plotted down the right hand margins of Figs 3 and 6. At very large time separations $\tau_x(t)$ should tend towards $\sqrt{2}\sigma_x$.

2.3 Radiosonde Measurement Errors

Each measured parameter is identified subsequently by the symbols; V for vector wind, T-temperature and Φ-geopotential.

For radiosonde observations at the standard pressure levels, the term E_x^2 has three components.

$$E_x^2 = (\varepsilon_p \cdot {}^{dX}/_{dP})^2 + \varepsilon_x^2 + R_x^2 \qquad 9$$

$\varepsilon_p({}^{dX}/_{dP})$ represents the RMS errors in x introduced by the errors in the radiosonde pressure measurements. ε_x represents the RMS errors in x introduced by the radiosonde sensing system other than by the mis-location in the vertical. R_x is the RMS uncertainty in x introduced by the limited resolution of the analysed data. The values of the first two terms on the R.H.S of equation 9 for V, T and Φ can be derived from the results of experiments performed by Edge et al, (1986) (see Table 1).

Table 1

Estimates of RS3 radiosonde standard level measurement errors

Pressure		Vector Wind				Temperature			Geopotential		
Level (hPa)	ε_p (hPa)	$({}^{dV}/_{dp})^*$	ε_v (ms^{-1})	$R_v^\dagger$ (ms^{-1})	E_v (ms^{-1})	$\sqrt{\varepsilon_T^2+\varepsilon_p\frac{dT}{dp}}$	$R_T^\dagger$ (°C)	E_T (°C)	ε_Φ (gpm)	$R_\Phi^\dagger$ (gpm)	E_Φ (gpm)
850	1.0	0.2	0.5	0.2	0.6	0.11	0.06	0.12	2.5	0.3	2.5
500	0.9	0.2	1.0	0.5	1.1	0.11	0.06	0.12	4.0	2.9	4.9
250	0.7	0.2	1.0	1.0	1.4	0.11	0.06	0.12	5.0	2.9	5.8
100	0.4	0.2	1.5	0.2	1.5	0.06	0.06	0.08	5.5	2.9	6.2
50	0.3	0.2	1.5	0.1	1.5	0.15	0.06	0.16	6.5	2.9	7.1

*Values are estimated only. †Values refer to analysis of TEMP or PILOT message data.

2.4 Variability Statistics

The statistics of vector wind variations are presented in Figs 1, 2, 3 and of temperature in Figs. 4, 5, 6.

In Figs 1 and 4 vertical profiles of $S_x(s)$ are presented for s equal to the minimum separation distance for stations in the synoptic radiosonde network (220 km) and for the minimum value of s from all available data (52 km). Similarly profiles of τ_x (t) were constructed, again for t characteristic of synoptic observations (12 hrs) and for the minimum t for which statistics were available. For comparison, profiles of the measurement error term $\sqrt{2}E_x$ have been included in these diagrams.

In a few cases at the smallest time and space separations considered, the measurement error term exceeded the contribution from atmospheric variability in equations 6 and 7. In these cases, reliable values of $S_x(s)$ and/or $\tau_x(t)$ could not be computed and hence have been omitted from

the diagrams. For temperature $F_x(s)$ rather than $S_x(s)$ is plotted to minimise any distortion due to climatological mean differences between the measurement sites.

3. OBSERVATIONAL ERRORS USED IN MODEL ANALYSIS

In order to make optimum use of observations in numerical analyses, the total uncertainty associated with the observation (the observational error) should be known. The observational error is a combination of the measurement error and a representativeness error which in turn is a function of the scales of atmospheric variations which can be resolved in the process of analysis.

In the analysis process use in the UK Meteorological Office operational global forecasting model the observations are compared to the value from the model 'background field' at the observation point. The significance of the difference is decided according to the magnitude of the observational error and the uncertainty in the background field. The observational error ($O_x(d)$) is defined by:-

$$O_x^2(d) = I_x^2(d) + E_x^2 \qquad 10$$

where $I_x(d)$ is the representativeness error appropriate for the model analysis; d is defined below.

It is possible to derive values of the observational error for the RS3 sonde appropriate for use in this quality control from the structure functions S(s) and $\tau(t)$. Consider an observation situated at the centre of a model grid-box. In the vicinity of the UK, the model grid-boxes have dimensions of approximately 130 x 170 km; for the purpose of estimating the representativeness error, it is assumed that the boxes are squares of side d=150 km. Then the error associated with interpolation of parameter x to the observation point from values of the model background field at the grid points is given by (see Gandin, 1970, Equation 32):-

$$I_x^2(d) = S_x^2\left(\frac{d}{\sqrt{2}}\right) - \frac{S_x^2(d)}{4} - \frac{S_x^2(d/\sqrt{2})}{8} \qquad 11$$

Note that errors in the model background field are considered to be zero at the grid points here because they do not contribute to the observational error as defined above. By solving equations 10 and 11,

estimates of the observational error may be obtained. However, such estimates would only apply to radiosonde observations located precisely at the point in space and time to which they are attributed in the model. In practice, two other factors need to be considered, namely:-

a) Radiosonde observations are attributed to the position of the launching site in the analysis, rather than the location of the observation.

b) It is a feature of the particular numerical model considered here that observations with nominal times of up to ±3 hours from the analysis time are all considered to have been made at the analysis time. This factor is of particular importance to data from those stations outside the synoptic network which make ascents on an irregular basis (see Section 2.1).

The above factors are incorporated into equation 10 by the addition of two extra terms.

$$O_x^2(d) = I_x^2(d) + S_x^2(\varepsilon_s) + \tau_x^2(\varepsilon_t) + E_x^2 \qquad 12$$

ε_s and ε_t here represent the displacement in space and time from the observation location assigned in the analysis. Table 2 lists four sets of ε_s and ε_t corresponding to "ideal" radiosonde observations, to extreme time displacement, to large spatial displacement typical of ascents through jet streams in the UK; and to more typical UK operational conditions. Equation 12 was evaluated for Cases 1-3 and d=150 km (for an observation assumed to be in the centre of a grid box) using the summer half-year structure functions. In Table 3, the results are compared to O_V and O_T which are in current operational use in the UK Meteorological Office model. These operational values are derived from studies of the observation-background fields and are applied to all radiosonde observations, not just those from the UK network (see Bell, 1985).

Table 2

Criteria used in the evaluation of Equation 12

Pressure Level (hPa)	Case 1 (Ideal)		Case 2 (Extreme time displ.)		Case 3 (Large horiz. displ.)		Typical UK conds.	
	ε_s	ε_t	ε_s	ε_t(hours)	ε_s(km)	ε_t	ε_s(km)	ε_t(hours)
850	0	0	0	3	5	0	0	.75
500	0	0	0	3	20	0	5	0.5
250	0	0	0	3	50	0	20	0.25
100	0	0	0	3	100	0	50	0
50	0	0	0	3	100	0	50	0.25

Table 3

Observational Error levels for RS3 observations used in the global model analysis.

Pressure	$O_v(ms^{-1})$				$O_T(°C)$				O_Φ(gpm)		
Level (hPa)	1	2	3	model	1	2	3	model*	1	2	3
850	3.1	4.6	-	2.5	0.6	1.2	-	1.1-1.5	6	9	-
500	3.5	5.1	-	3.1	0.9	1.3	-	0.8-1.1	12	18	-
250	4.8	7.5	5.6	4.7	1.3	2.0	1.5	1.1-1.5	19	28	-
100	2.7	-	3.9	3.5	1.0	1.6	1.5	1.2-1.6	12	16	18
50	2.6	-	3.7	3.5	0.8	1.3	1.3	1.3-1.7	14	18	21

*Exact figure depends upon assessment of temperature data quality for individual radiosonde stations. Stations in UK synoptic network fall within band indicated.

Blanks indicate values cannot be computed from available data.

The magnitudes of O_v and O_T currently used in observation quality control for the model generally agree to within a factor of 2 with our experimentally derived values except for stratospheric temperatures. Uncorrected radiation errors in radiosonde measurements at upper levels can be up to about 2°C for some radiosonde designs (although not for the RS3, see Nash and Schmidlin, 1987) and observational error levels in the model analysis reflect this level of uncertainty in the temperature measurements.

The differences between the results from the three cases are significant. The effect of large horizontal displacements (Case 3) is to increase the temperature errors by about 50% over that of the ideal (Case 1) in the stratosphere. This result suggests that a further reduction in the model values of observational errors could be achieved by ascribing the radiosonde observations to the correct position. It is recognized that the structure functions $S_x(s)$ used in this analysis are derived from data for displacements randomly orientated with respect to the gradients at a particular level in the atmosphere, whereas the balloon displacements are always along wind. Thus, observational errors for Case 3 may be overestimated here. The effect of the largest time displacement is similar, increases over Case 1 again being about 50%.

4. CONCLUSIONS

a) Statistics of the differences between radiosonde observations separated in space and time have been used to determine atmospheric structure functions which have a number of applications.

b) The high reproducibility of the UK RS3 radiosonde ensures that measurement errors are confined to an acceptably low level when considering analysis of temperature, geopotential and wind fields on the synoptic scale. Limitations imposed by the radiosonde upon the estimation of gradients on isobaric surfaces only become evident when observation separation is reduced to a few tens of kilometres and/or a few hours. Observation errors associated with the synoptic scale analysis of high quality radiosonde measurements are dominated by the representativeness errors. Thus the reproducibility of the measurements cannot be determined directly from observation error statistics.

c) The total observational error associated with the use of RS3 radiosonde data in synoptic analysis could be reduced in some cases if the observations were attributed to the correct location rather than the launch site. Similarly, the use of asynoptic radiosonde data with a nominal ascent time of up to 3 hours from the analysis time increases the observational error level significantly.

If current trends are maintained towards higher spatial and temporal resolution in meteorological analysis, and more reproducible radiosonde system measurements, then the need for refinement of observing practices will inevitably increase.

References

Bell R.S., 1985: Operational numerical weather prediction system documentation paper No 3 - The data assimilation scheme, Ed. R.R. Bell, Meteorological Office, Bracknell.

Edge P., Kitchen M., Harding J.H. and Stancombe J., 1986: The reproducibility of RS3 radiosonde and Cossor WF Mk IV radar measurements, OSM 35, Meteorological Office, Bracknell.

Gandin L.S., 1970: The planning of meteorological station networks. WMO Technical Note 111, WMO, Geneva.

Morgan J.,1984: The accuracy of SATOB cloud motion vectors. ECMWF Workshop on the Use and Quality Control of Meteorological Observations. 6-9 November 1984, 137-169, ECMWF, Reading.

Nash J. and Schmidlin F.J., 1987: Final report on the WMO International radiosonde comparisons, Instruments and Methods of observation, Report No 30. WMO, Geneva

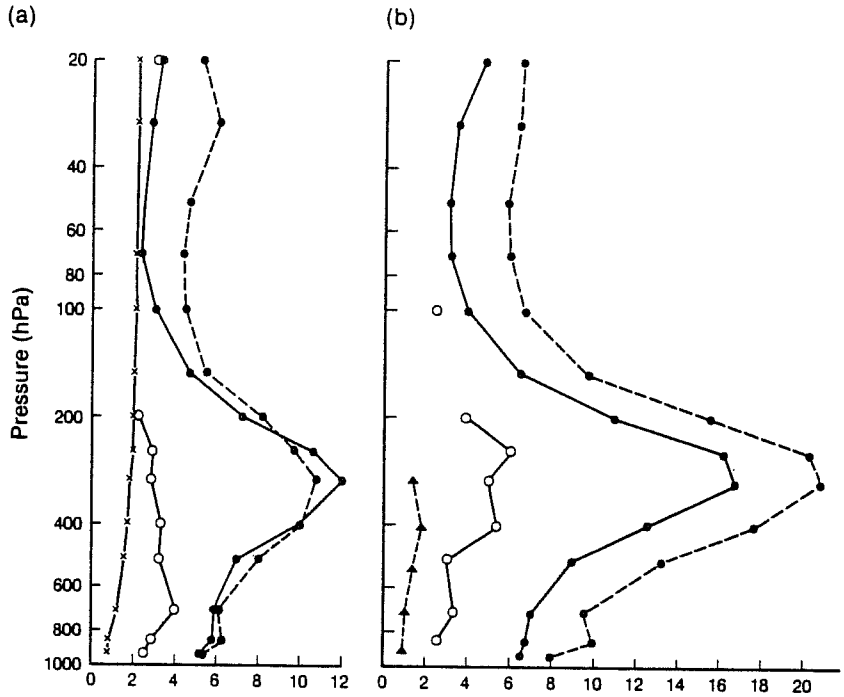

Fig. 1.
Profiles of the RMS difference between vector wind observations at standard pressure levels separated by distance s or time interval t.
Fig. 1a ×—× $-\sqrt{2}E_V$, ●—● $-S_V$(s=220 km), ○—○ $-S_V$(s=52 km)
Fig. 1b ●—● $-\tau_V$ (t=12 hours), ○—○ $-\tau_V$ (t=2 hours), ▲---▲ $-\tau_V$ (t=3 hours)
Points joined by solid lines refer to summer half-year data, those joined by dotted lines refer to winter half-year data.

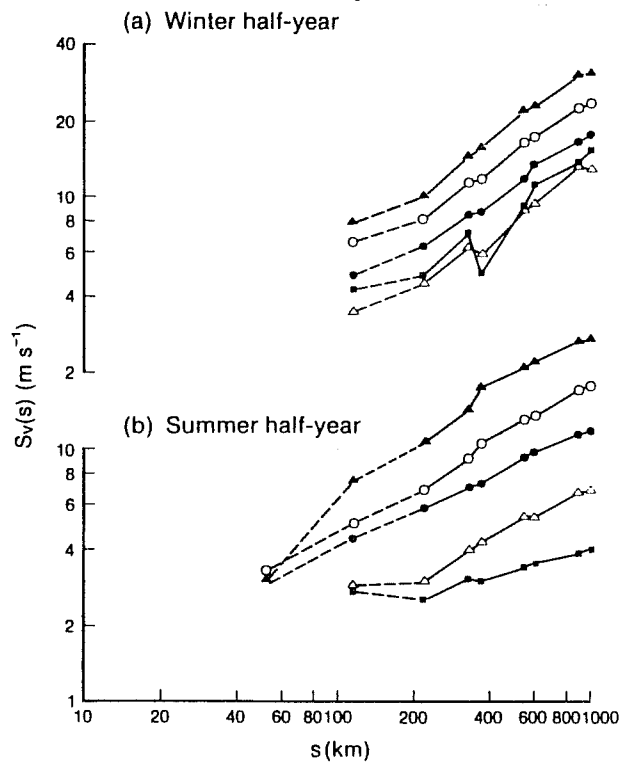

Fig. 2.
RMS differences between measurements of vector wind separated by a distance s (spatial structure functions) at 5 standard pressure levels. ● -850hPa ○ -500hPa ▲ -250hPa △ -100hPa ■ -50hPa. Fig. 2a is for the winter half-year and Fig. 2b is for the summer half-year.

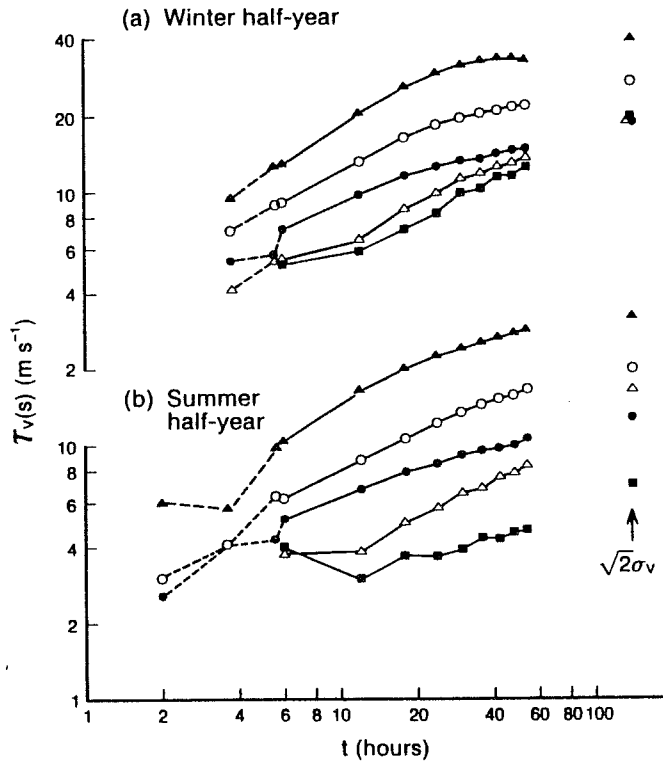

Fig. 3.
RMS differences between measurements of vector wind separated by a time interval t (temporal structure functions) at the same 5 pressure levels as in Fig. 2. Values of $\sqrt{2}\sigma_V$ are plotted down the RHS of the graph outside the axes.

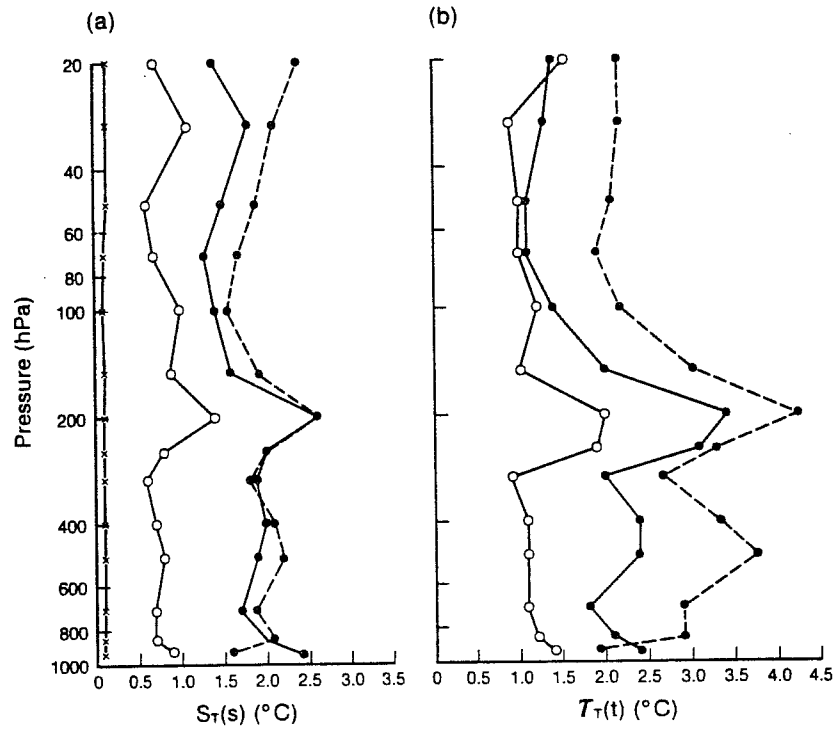

Fig. 4.
Similar to Fig. 1 but for temperature.
Fig. 4a ×—× $-\sqrt{2}E_T$, ●—● $-S_T(s=220km)$, o—o $-S_T(s=52km)$.
Fig. 4b ●—● $-\tau_T(t=12hours)$, o—o $-\tau_T(t=4$ hours)

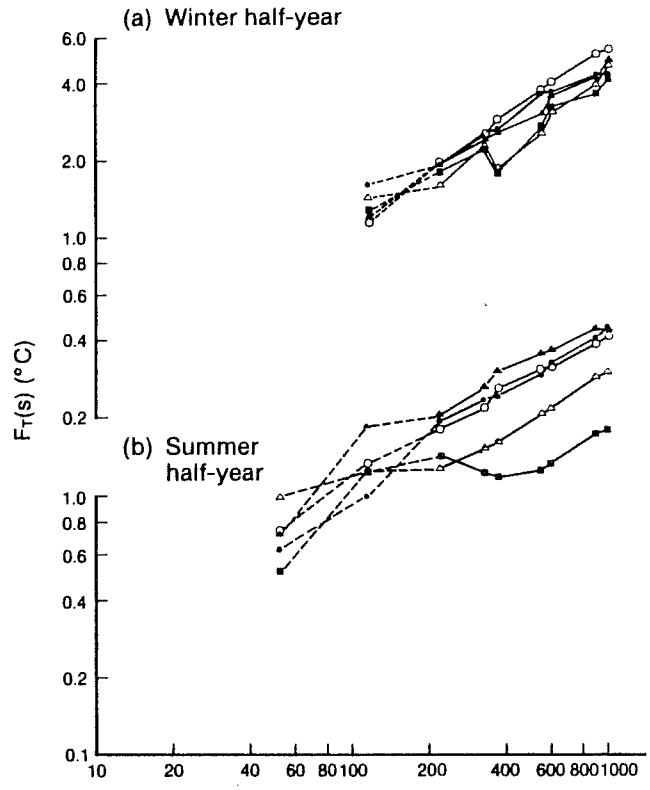

Fig. 5.
Similar to Fig. 2 but showing spatial structure functions for measurements of temperature at the same 5 standard pressure levels. $F_T(s)$ rather than $S_T(s)$ is the variable plotted.

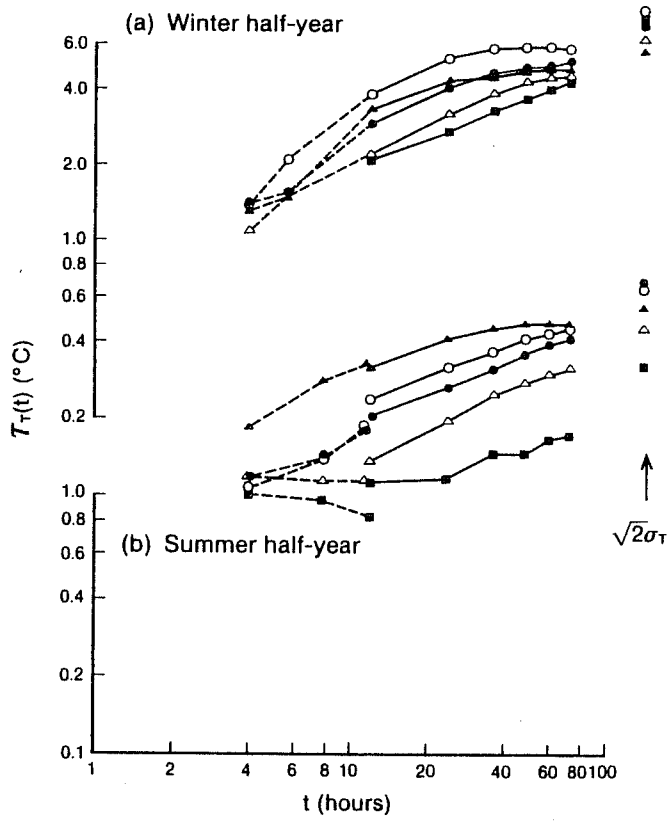

Fig. 6.
Similar to Fig. 3 but showing temporal structure functions for temperature measurements.